POWDER RHEOLOGY AND COMPACTION BEHAVIOUR OF SPRAY-DRIED BODIES FOR PORCELAIN STONEWARE SLABS

Roberto Soldati[1], Chiara Zanelli[1], Guia Guarini[1], Sandra Fazio[2], Maria Chiara Bignozzi[2], Michele Dondi[1]

[1]CNR-ISTEC, via Granarolo 64, Faenza, Italy

[2]Centro Ceramico, via Martelli 26/A, Bologna, Italy

1. ABSTRACT

The technological behaviour of porcelain stoneware bodies during deposition and pressing of large slabs depends on the rheological properties of spray-dried powders and the way they affect compaction. Although the literature offers some insights into the characteristics of spray-dried powders for ceramic tiles, no data are available on bodies used by novel technologies for large slabs (>4 m^2). In order to fill this gap, a systematic approach to properties and behaviour of spray-dried powders for porcelain stoneware slabs was carried out. For this purpose, 11 industrially-manufactured spray-dried powders were characterised for their intrinsic features (particle size and agglomerate size distribution; shape and moisture distribution in function of agglomerate size); rheological properties (mass flow, static and dynamic angles of repose, poured and tapped density); compaction behaviour (curves of bulk density, intergranular and intragranular porosity in function of applied load); and firing behaviour, in order to reveal any effect of dry bulk density on shrinkage and bulk density of fired samples. The effect of these intrinsic characteristics on the flowability and

compressibility of powders was appraised, as was the mutual relationships between the rheological parameters. Two broad classes of spray-dried powders occur with a finer and a coarser agglomerate size distribution. Results reveal that ceramic powders are free-flowing, with rheological properties fluctuating in a rather narrow range of values, which makes hard to see strict correlations between the various methods. Flowability mainly depends on the occurrence of coarser aggregates, particularly those irregular in shape, stemming from coalescence of three or more individual agglomerates. The features of green compacts are somehow inherited by the fired bodies, especially in terms of shrinkage and densification kinetics, even though the starting differences are damped during firing. The performance of spray-dried bodies during compaction is crucial to control uniformity, in terms of porosity and bulk density, which has important repercussions on the properties of final slabs, especially considering that residual stresses may be related to differential shrinkages during firing due to density gradients.

2. INTRODUCTION

The manner in which spray-dried powders flow through the way out of hoppers and deposit into a die or on a tape affects the structure of green tiles, particularly their bulk density and mechanical strength [1, 2]. This behaviour somehow depends on the characteristics of spray-dried powders, namely agglomerate size distribution, shapes of granules and moisture distribution in function of the agglomerate size.

For these reasons, there is a growing concern in the ceramic industry regarding rheological properties of spray-dried powders that can suitably represent their behaviour during deposition and compaction, especially in the case of large slabs [3, 4]. Powder rheology can be measured by different methods [5, 6, 7]. The most popular include: static angle of repose [8-11]; dynamic angle of repose [12]; poured density, tapped density and Hausner ratio [8, 11, 13, 14]; and mass flow through an orifice [6].

Powder compaction is a key step in ceramic tile manufacturing. It governs the amount and spatial distribution of porosity in the green and dry semi-finished products. These features control the mechanical strength of unfired tiles, as well as the firing shrinkage and final microstructure in terms of residual porosity [15, 16]. This is particularly true in case of large slabs obtained with novel compaction technologies [3, 4, 17], and for thin or very thick tiles [18, 19]. The pressing behaviour of ceramic bodies depends on both the characteristics of spray-dried powders (agglomerate size distribution, granule shape and mechanical resistance, porosity) and the way they fill the die (or lay on the tape) and rearrange under increasing pressure [20, 21].

In the ceramic tile sector, little attention has been paid to spray-dried powder features: initially for red stoneware [22, 23] and then for porcelain stoneware tiles [24, 25]. A picture of the rheological behaviour of spray-dried powders actually used in the manufacture of large porcelain stoneware slabs is still missing. On the other hand, the compaction behaviour of spray-dried powders has been, for a long time, a target of research for advanced ceramics [20, 21, 26, 27] as well as for ceramic tiles [1, 2, 22, 28]. Nevertheless, the concern regarding porcelain stoneware bodies has grown in the last decade [2, 24, 25, 29-32]. This literature provides data on agglomerate size distribution, porosity, mechanical strength and microstructure of spray-dried powders, along with compaction curves and characteristics of pressed tiles (e.g., bulk density, anisotropy, microstructure, pore size distribution) and their dependence on processing parameters.

The scope of this preliminary contribution is to outline the main rheological characteristics of industrial bodies, and to draw a picture of the compaction behaviour of spray-dried powders used to manufacture large slabs of porcelain stoneware. The goals are i) to understand which parameters are significant in case of large slabs of porcelain stoneware , and ii) to build a database for modelling the rheological behaviour of spray-dried ceramic powders.

3. EXPERIMENTAL

Eleven spray-dried powders of porcelain stoneware bodies, currently used in the manufacturing of large slabs, were sampled and characterised for physical and rheological properties. The determined powder characteristics are: agglomerate size distribution by dry sieving (meshes from 1 to 0.1 mm), shape of granules (optical microscopy on sieve fractions with modal analysis on micrographs), and moisture distribution in function of the agglomerate size (weight difference of wet and dry fractions for each sieve).

Powder rheology was investigated by determining (Fig. 1): static angle of repose, α_{sta} [9] and dynamic angle of repose, α_{dyn} [12]; poured density (ρ_{pou}), tap density (ρ_{tap}) and Hausner ratio, HR [8]; mass flow rate (M_{FR}) by using a Ford cup.

The compaction behaviour was investigated in function of uniaxial pressure up to approximately 800 kg cm^{-2} (80 MPa) with laboratory hydraulic presses. Molds had dimension L_m from 50 mm (diameter) to 110x55 mm. As-pressed specimens were characterised by measuring weight and dimensions (length x width x thickness = volume). Green bulk density was obtained by the weight/volume ratio. The Carr compressibility index was calculated as $CI=100\cdot(V_m-V_p)/V_m$, where V_m is the volume of the die filled by powder and V_p is the volume of the pressed specimen.

The microstructural evolution with pressure was followed through observation of the normal surface to the pressing axis under optical microscope. The volume of the internal cavity of spray-dried powders was estimated on four size fractions by cutting the agglomerates, previously glued on a paperboard, and measuring the relative size of the granule and the cavity by optical microscopy.

The pore size distribution of the spray-dried powder and specimens pressed at 50, 75, 150 and 300 kg cm^{-2} was assessed. Specimens were previously dried in an oven, by Mercury Intrusion Porosimetry (MIP) up to 2 kbar (corresponding to a pore diameter of ~50 nm). Along with pore size, pore volume (PV), bulk density (BD) and open porosity were determined. Sample compression (Cp) during testing, calculated as Cp=PV-[(1/BD)-(1-RD)], was attributed mainly to collapse of the internal cavity. The real density (RD) of the bodies was determined by Helium pycnometry.

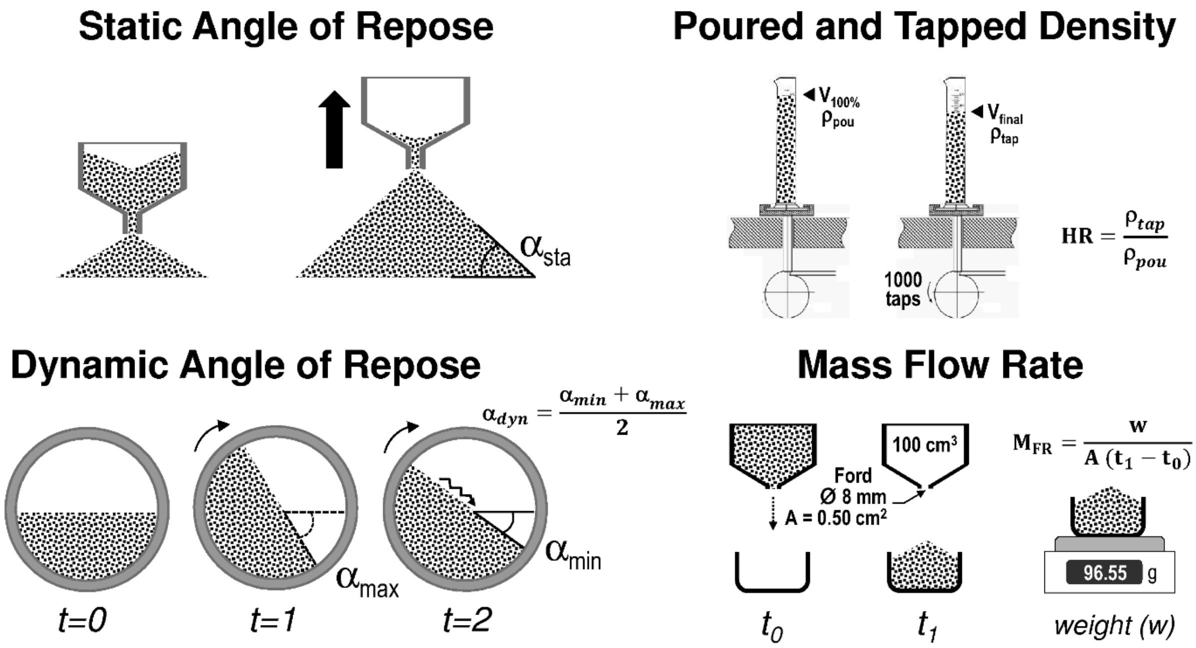

Figure 1. *Methods followed to determine the rheological properties of spray-dried powders.*

4. RESULTS AND DISCUSSION

Characteristics of spray-dried powders

Agglomerate size distribution of porcelain stoneware bodies is shown in Figure 2. Two kinds of distribution are visible: finer-grained powders (mean size around 250 μm) and coarser-grained powders (mean size ~350 μm). This contribution is focused on the comparison of two samples, which are representative of finer-grained and coarser-grained powders respectively.

Moisture varies according to agglomerate size (Fig. 3). There is an overall trend of growing moisture with the increase on granule size. For this reason, on average, finer-grained powders are slightly less humid than coarser-grained ones (Table I). Although this is an expected trend, current data allow to size the difference in moisture, e.g. between 400-500 μm and 100-200 μm fractions, into about 2% (single values spanning from 0.5% to 4.5%). However, sometimes there are fluctuations in intermediate size fractions and even cases of flat distribution with maximum moisture in the finest fraction.

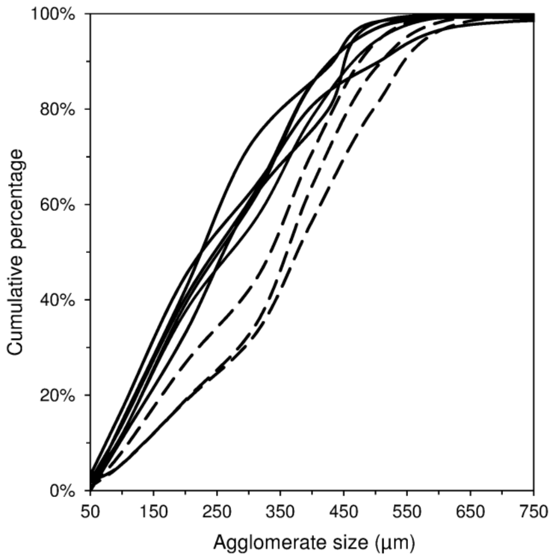

Figure 2. *Agglomerate size distribution of porcelain stoneware bodies (dashed line = coarser-grained).*

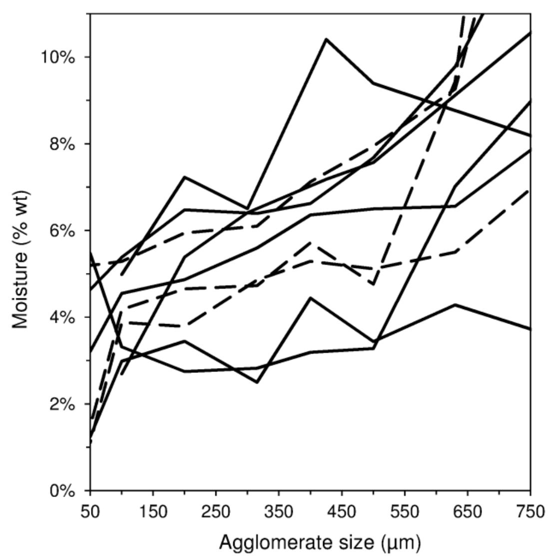

Figure 3. *Moisture distribution according to agglomerate size in porcelain stoneware bodies.*

Parameter	Unit	Finer-grained powders			Coarser-grained powders		
		min	MAX	**mean**	min	MAX	**mean**
Mean size of agglomerates	µm	225	270	**247**	335	375	**358**
Agglomerates larger than 500 µm	wt%	2.2	15.0	**6.4**	5.8	23.1	**15.8**
Agglomerates with "popcorn" shape	wt%	4.1	36.7	**16.6**	15.9	34.2	**28.0**
Moisture of spray-dried powders	wt%	3.2	6.1	**4.8**	4.5	7.2	**6.0**
Static angle of repose, $\checkmark_{sta}$	°	25	34	**30**	30	34	**32**
Dynamic angle of repose, $\checkmark_{dyn}$	°	34	45	**39**	34	43	**38**
Mass flow rate, M_{FR}	$g{\cdot}cm^{-2}{\cdot}s^{-1}$	13.3	15.9	**14.8**	13.5	15.0	**14.1**
Poured density, $\times_{pou}$	$g{\cdot}cm^{-3}$	0.93	1.01	**0.98**	0.95	1.05	**0.98**
Tapped density, $\times_{tap}$	$g{\cdot}cm^{-3}$	1.03	1.12	**1.10**	1.04	1.12	**1.10**
Hausner ratio, HR	1	1.09	1.17	**1.12**	1.07	1.15	**1.12**

Table I. *Characteristics and rheological behaviour of spray-dried powders.*

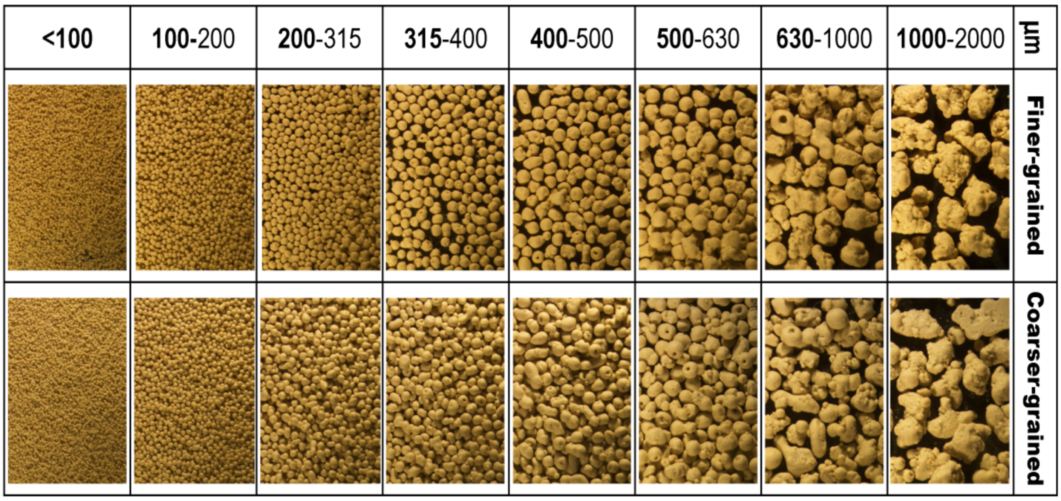

Figure 4. *Shapes of spray-dried granules in the various size fractions*

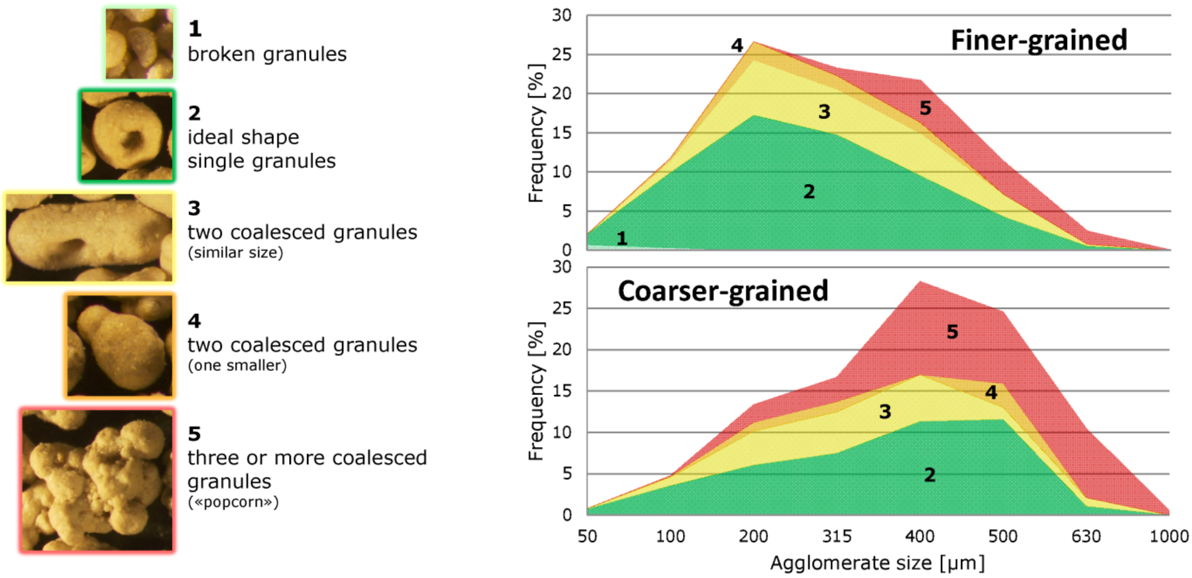

Figure 5. *Granule morphology is defined according to five basic shapes (left). Agglomerate shape distribution: examples for finer-grained and coarser-grained spray-dried powders (right).*

Agglomerates exhibit diverse shapes that occur with a variable frequency in the different size fractions (Fig. 4). Such shapes can be attributed to the ideal morphology of spray-dried granules, but also to further cases, such as broken granules or coalescence of two or more granules (Fig. 5). Shape distribution varies widely according to agglomerate dimension, even though a general trend arose: the "popcorn"-shaped granules occur essentially in the coarsest fractions (>400 µm) as the "twinned" granules (morphologies 3 and 4 in Fig. 5) are more frequent in the intermediate fractions (200-500 µm).

However, this general picture, outlined in Figure 5 for finer-grained and coarser-grained powders, is not systematic. Significant changes may occur according to powder treatment (spray-drying, storage, possible re-moisturising or dew) [1].

Rheological properties of spray-dried powders

Values measured for the rheological properties of finer-grained and coarser-grained powders are summarised in Table I. Both the static and dynamic angles of repose vary in a rather narrow range (25-34° α_{sta} and 34-45° α_{dyn}) with the fields of finer-grained and coarser-grained powders substantially overlapped. This circumstance makes it difficult to have a clear discrimination of flowability by the angle of repose; the experimental uncertainty is around 1°, considering the bias caused by the occurrence of a lower angle and an upper angle, which is not a trivial distinction. In case of the static angle of repose, the measured values correspond to "free-flowing" powders [8]. Very low values (<30°), referred to as "excellent flowing", seem to only be achievable by some finer-grained, spray-dried bodies.

The interval of mass flow rate is practically the same (13-16 $g \cdot cm^{-2} \cdot s^{-1}$) for finer-grained and coarser-grained powders (Table I) when a relatively wide orifice is used (8 mm in diameter). Mass flow decreases by reducing orifice light (e.g., 6 mm or 4 mm), but no discrimination is achieved in terms of powder flowability.

Poured density varies from 0.93 to 1.05 $g \cdot cm^{-3}$, with a mean value around 0.98 $g \cdot cm^{-3}$ for both finer-grained and coarser-grained powders, even though it seems that the highest densities are obtained with some of the finer bodies (Table I). It must be emphasised that this apparently simple determination is, in reality, tremendously affected by the experimental conditions (e.g., height of fall, geometry of container, filling rate) and thus, dependent on the analyst to a good extent.

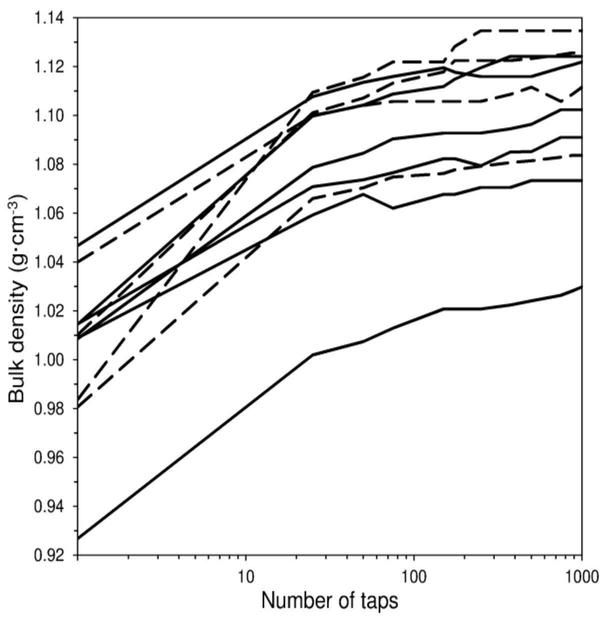

Figure 6. *Bulk density curves according to taps for coarser-grained (dashed lines) and finer-grained powders.*

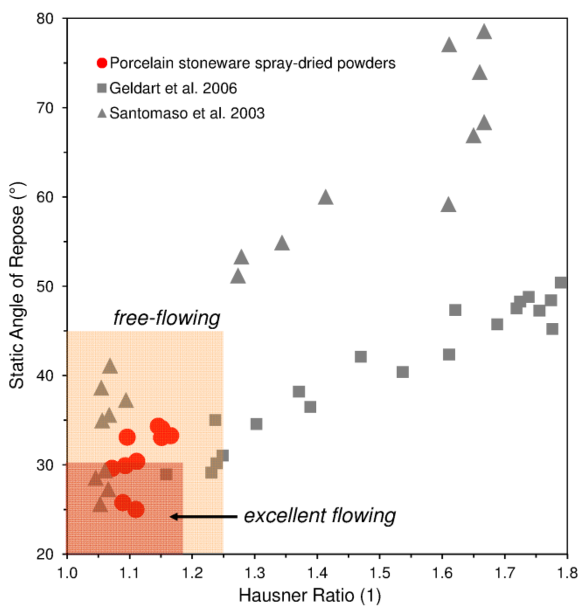

Figure 7. *Correlation of Hausner ratio versus the static angle of repose for ceramic powders compared to other kinds of powders [8, 9].*

The finer-grained and coarser-grained powders exhibit the same interval of values (1.03-1.12 $g\cdot cm^{-3}$) for the tapped density (Table I). Nevertheless, different packing curves are observed (Fig. 6). Packing efficiency is connected to the agglomerate size distribution and, particularly, to a favourable ratio of coarse and fine dimensions [33, 34].

Overall, the Hausner ratio ranges from 1.07 to 1.17, as there is no significant difference between finer-grained and coarser-grained powders (Table I). All these values are below 1.25, so they correspond to "free-flowing" powders [8]. In reality, most spray-dried bodies exhibit HR<1.15, and thus, they can be considered powders with "excellent flowing". The expected relationship between Hausner ratio and angle of repose apparently does not hold for ceramic powders, because the variation ranges of both HR and α_{sta} are too small to allow any clear trend, as those observable with a wide set of different powders (Fig. 7).

Physical characteristics of spray-dried powders are contrasted with their rheological properties in a matrix of binary correlations (Fig. 8). Some relationships stand out with a similar trend for the agglomerate size and shape, particularly the coarse fraction (>500 μm) and the percentage of "popcorn"-shaped granules. The same trends are perceivable for the average size of agglomerates, but with a scarce significance.

Both the static and dynamic angles of repose are directly related to agglomerate size and shape: the larger the amount of coarse and "popcorn"-shaped granules, the higher α_{sta} and α_{dyn}.

Mass flow rate increases as the average size of agglomerates decreases. This tendency is clearly dependent on the percentage of coarse and irregularly-shaped granules.

Poured density correlates with spray-dried powders features in a complex way, and thus, broad distributions can be often observed in Figure 8. At any rate, ρ_{pou} is higher when the amount of coarse granules is <10%.

Tapped density appears to be independent from the characteristics considered here for spray-dried powders. However, the packing efficiency of granules depends on the ratios between coarse, fine and intermediate size fractions [33, 34], hence why deeper data elaboration is necessary to reveal if this also holds true for ceramic powders.

Broad trends arose for the Hausner ratio, especially some direct correlation with the amount of coarse and "popcorn"-shaped granules.

Moisture does not to affect significantly the rheological behaviour of powders. Perhaps the only exception was the mass flow rate, which exhibits a trend analogous to those observed in comparison with the agglomerate size and shape. This statement is valid only for the moisture interval of the samples under investigation.

Overall, the most significant correlations are with the percentage of coarse and irregularly-shaped granules: positive for the Hausner ratio and the angle of repose, negative for the mass flow rate and the poured density. All these tendencies converge towards lower flowability of the powders containing more "popcorn"-shaped granules and/or agglomerates over 500 μm.

This observation has repercussions on the modelling of the spatial arrangement of spray-dried powders [35, 36]. The main deviation from the predictable flowability, in fact, is connected to the occurrence of irregular and coarse aggregates.

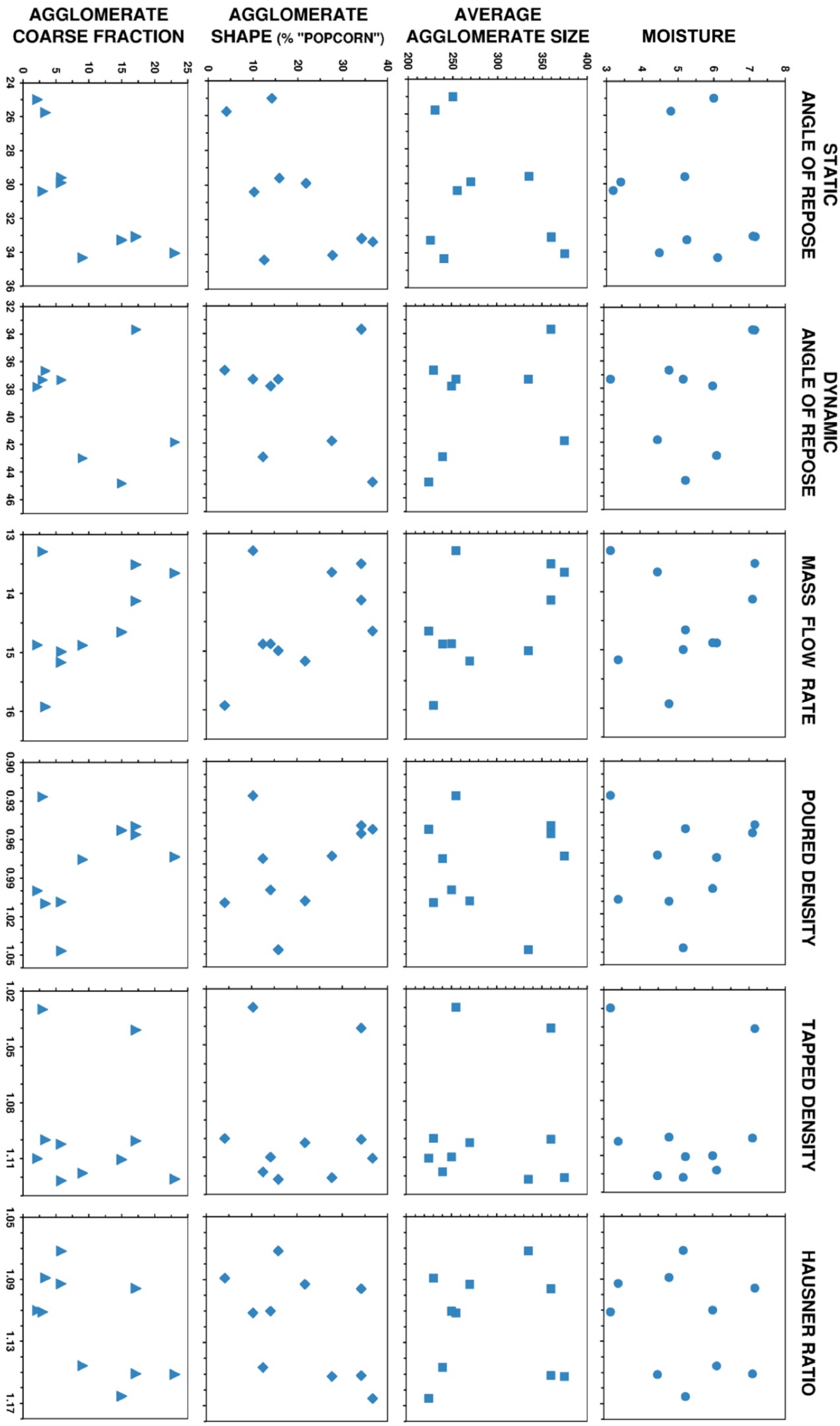

***Figure 8**. Correlation matrix of spray-dried powder characteristics (agglomerate size, shape and moisture) versus the main rheological parameters (static and dynamic angle of repose, mass flow rate, poured and tapped density, Hausner ratio).*

Compaction behaviour of spray-dried powders

A starting situation is envisaged as agglomerates fill a die or are deposited as soft layer on a tape (Fig. 9). Different types of porosity can be distinguished: intergranular and intragranular (both micro- and macro-porosity). Intragranular microporosity is represented by micrometer-sized pores, which can be either incompressible (P_{1a}) or compressible (P_{1b}) under the pressures usually applied in tile making. Intragranular macroporosity is characteristic of spray-dried granules: it consists of a nearly spherical cavity (P_{2a}) and a funnel (P_{2b}) connecting the cavity with the outer surface. Intergranular porosity (P_3) depends on the packing efficiency of granules during deposition on the tape or into the die.

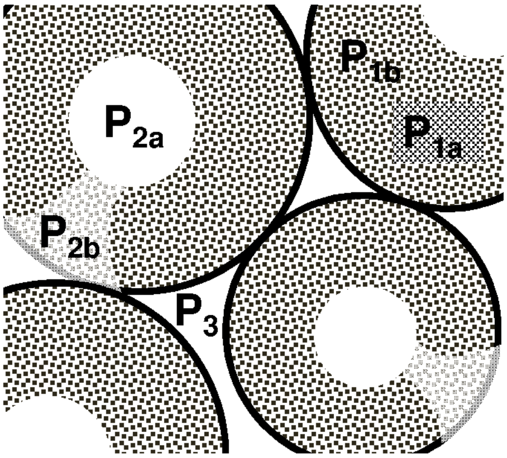

Figure 9. *Different types of porosity in the soft powder layer. Intragranular micro-porosity: incompressible (P_{1a}) and compressible (P_{1b}); intragranular macro-porosity: cavity (P_{2a}) and funnel (P_{2b}); intergranular porosity (P_3).*

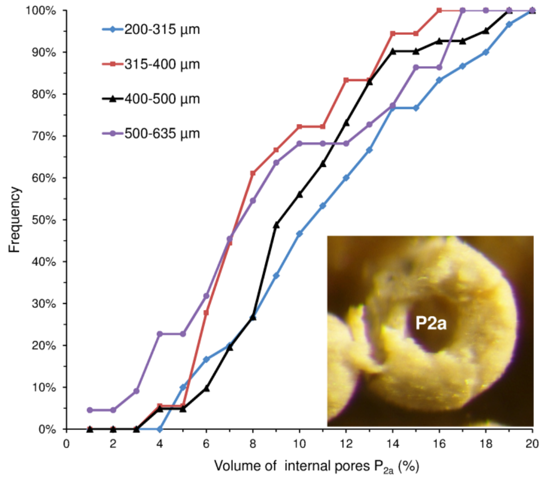

Figure 10. *Relative volume of intragranular porosity P_{2a} in granules of different size.*

Relative volume of intragranular porosity (P_{2a}) is on average 10% of the granule volume, regardless of agglomerate size, with almost all values between 5% and 15% (Fig. 10). These data are consistent with previous estimates [1, 24], even though the estimates are, of course, only valid in cases of ideal morphology of spray-dried granules.

The compaction of spray-dried powders with increasing pressure brings about a clear change in microstructure. Intergranular porosity (P_3) closes progressively and single granules are squeezed to form triple joints, where some residual pores persist over 150 kg cm^{-2} (Fig. 11).

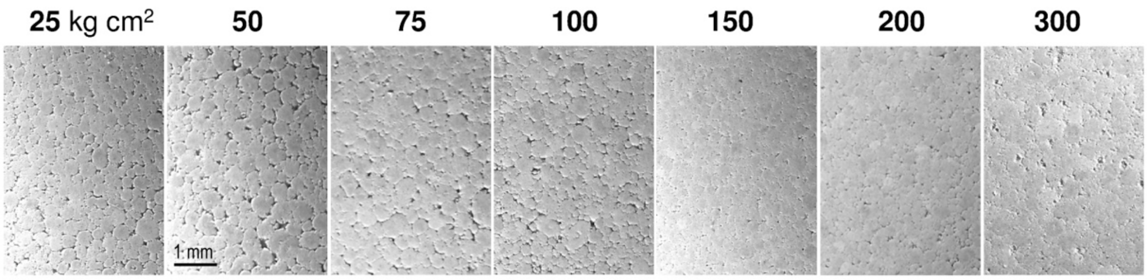

Figure 11. *Surface microstructure of compacts pressed at increasing pressures.*

The resulting bulk density curves compared with the pressure outline two compaction regimes: first, a density that rapidly increases up to approximately 13 MPa, followed at higher pressures by a slow gain in density (Fig. 12A). The occurrence of an abrupt switch between the two regimes is only apparent (as it was not possible to collect data below 13 MPa in the test with laboratory press). In reality, a gradual transition zone stands out once the test is carried out in a single run (see inset in Fig. 12A). Overall, the curves seem to correspond to the pressing behaviour of spray-dried powder that contains aggregates which can be broken during compaction [21]. Interestingly, coarser-grained powders tend to compact more than finer-grained ones, even though there are exceptions (Fig. 12B). This is related to the different moisture distribution, inasmuch the coarser-grained powders are more humid.

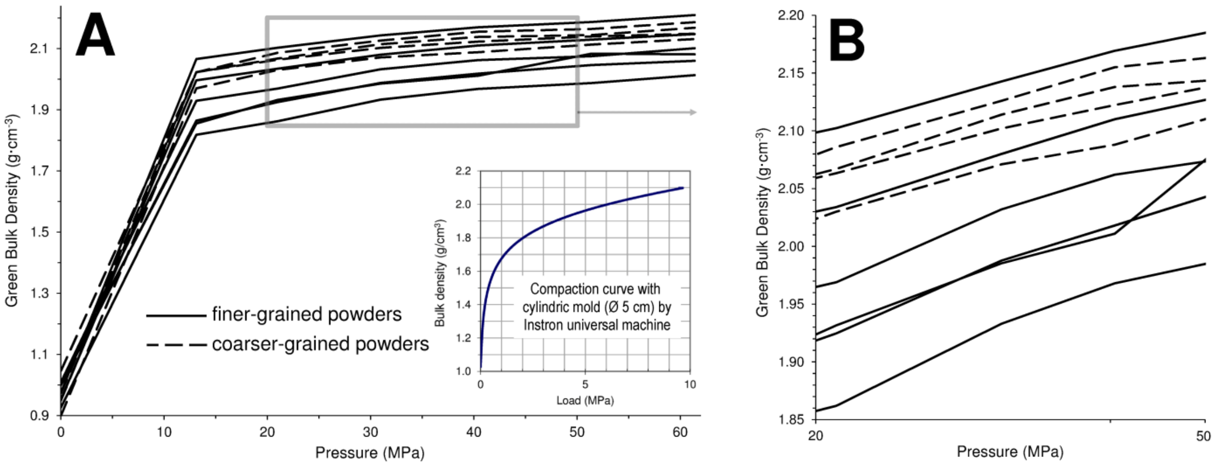

Figure 12. *Compaction curves of spray-dried powders by testing specimens shaped with a laboratory press compared to a single run (A); detailed comparison with pressure in logarithmic scale (B).*

Compressibility of spray-dried powders, expressed by the Carr index at 40 MPa of pressure, ranges from 50% to 58%, with most samples between 50% and 55%.

The two compaction regimes can be related to the work needed to compress the different types of porosity described in Figure 1. The evolution of porosity with increasing pressure was quantitatively inferred by mercury intrusion porosimetry: cumulative curves and histograms of pore size distribution are shown in Figure 13 for the low-P regime (50 and 75 kg cm^{-2}), the high-P regime (300 kg cm^{-2}) and the transition zone (150 kg cm^{-2}).

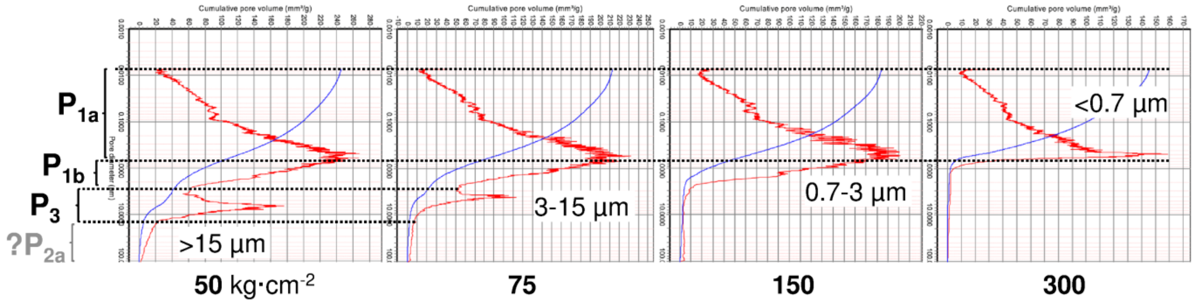

Figure 13. *Pore size distribution curves (cumulative and pore volume by mercury intrusion porosimetry) according to pressure (from 50 to 300 kg cm^{-2}). Pore types are related to pore size ranges.*

Comparing pore size curves, the progressive reduction of macropores can be observed (i.e., the pore population in the 3-15 µm range, peaking at ~8 µm) by increasing pressure from 50 to 150 kg cm^{-2}, where they practically disappeared. This pore population is attributable to the intergranular porosity P_3. Its gradual closure corresponds to the steep slope of compaction curves (the low-P regime).

The broad range of micropores present in the granules (going from ~3 µm to 50 nm) gradually narrows at higher pressures. By this way, the coarser micropores, which vary approximately from 3 to 0.7 µm, are completely downsized at 300 kg cm^{-2}. This is mirrored by the lazy slope of compaction curves over 150 kg cm^{-2} (the high-P regime).

Evolution of the different types of porosity present in the soft layer of spray-dried powders can be inferred by crisscrossing data from mercury intrusion porosimetry, poured density and optical microscopy (Fig. 14). Intergranular porosity P_3 rapidly closes in the early stages of compaction, having almost completely disappeared at 150 kg cm^{-2}. The internal cavity is apparently splashed at very low pressure (<50 kg cm^{-2}).

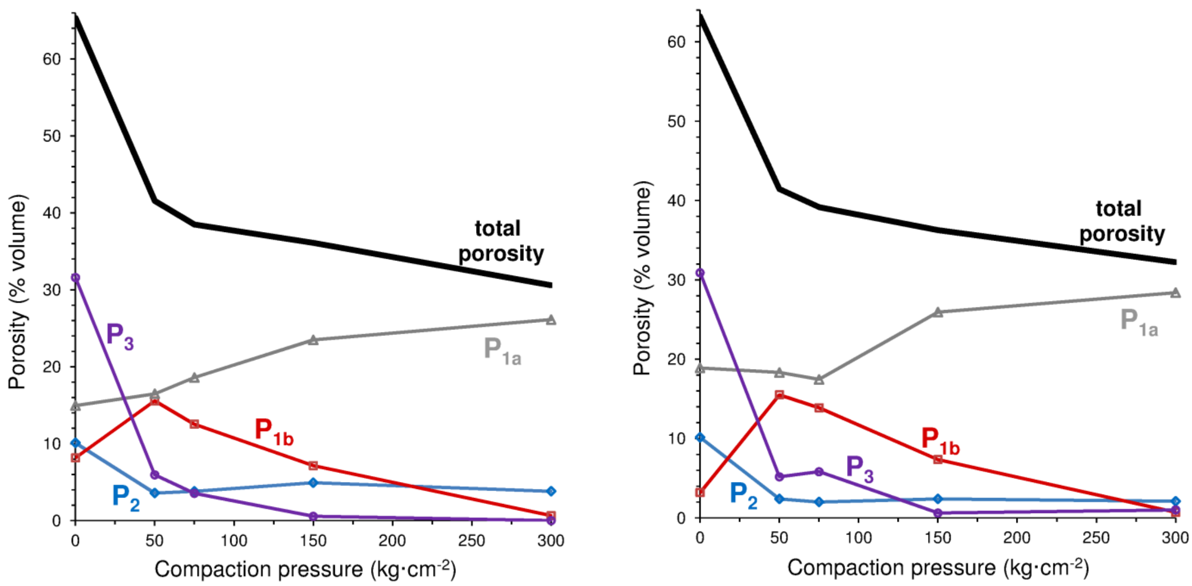

Figure 14. *Variation of different types of porosity in the soft layer of spray-dried powders (see Fig. 9) according to the pressure on finer-grained powders (left) and coarser-grained powders (right).*

Nevertheless, a residual porosity P2 that could be attributed to the funnel is still perceivable at high pressure. Increasing compaction with pressure proceeds through the downsizing of porosity, firstly P2 and P3, which brings about an increase of the coarser fraction of micropores (P1b) at 50 kg cm-2. With the growing pressure, compressible micropores (P1b) are progressively converted into the incompressible fraction (P1a).

Pressure acts simultaneously on the different types of porosity: P2a and P3 are closed (and to some extent downsized to P1b) in the low-P regime, while in the high-P regime the compressible pores (P1b , and perhaps the funnel P2b), are downsized to P1a.

Saturation of pores by water can be estimated when assuming that the initial moisture of the spray-dried powder is essentially contained in the micro-porosity and entirely retained during pressing. In this case, the starting pore saturation (volume occupied by water out of total micropores volume) is around 19-21% (for spray-dried powders with 6-7% moisture). Such saturation degree increases to 23-25% in the tile pressed at 300 kg cm-2 and it shall be slightly more at usual industrial pressure (~400 kg cm-2).

These findings carry implications for compaction modelling: it should take into account a change, with increasing pressure, in the mechanical response of spray-dried granules. In fact, the agglomerates turn increasingly stiffer once the intergranular porosity and their internal cavity are closed, and work is performed to downsize the compressible micro-porosity.

A different degree of compaction might be present in unfired slabs, e.g., as values of dry bulk density changing from point to point. However, differences in dry bulk density are damped during firing, because a more porous body sinters faster than a less porous one [37]. This phenomenon can be observed when considering two spray-dried powders (finer-grained and coarser-grained, respectively, i.e. the two denser in Fig. 12) that were compacted at increasing pressures from 13 to 80 MPa. Thus, a range of dry bulk density was achieved: 1.90-2.03 g cm-3 (coarser-grained body) and 1.94-2.08 g cm-3 (finer-grained one); the overall range is 0.13-0.14 g cm-3. These values are contrasted with the bulk density of the corresponding specimens, fired with an industrial-like schedule, plotting data with the same scale (Fig. 15). The bodies shrank during firing, attaining a bulk density as high as 2.32-2.36 g cm-3 (coarser-grained body) and 2.35-2.37 g cm-3 (finer-grained one); the overall range is 0.02-0.04 g cm-3. At lower dry bulk density, larger firing shrinkage.

If the difference in bulk density for two parts of the same unfired slab is expressed as 100%, such gap turns to be just 15% to 30% after firing. Thus, 70% to 85% of the initial difference is recovered in a different shrinkage during the sintering process. This implies that any difference in dry bulk density is paid in terms of differential shrinkage, which may be dangerous, being a probable cause of permanent deformation and residual stress after firing [38-40].

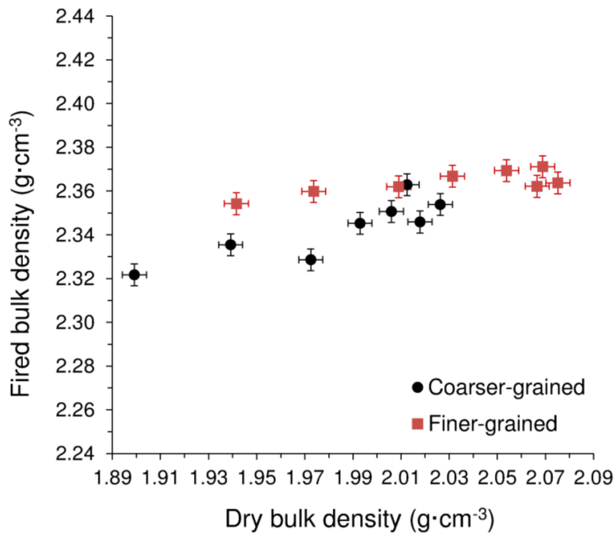

Figure 15. *Bulk density in fired and unfired porcelain stoneware tiles pressed from 13 to 80 MPa. Two bodies with different agglomerate size distribution are compared.*

5. CONCLUSIONS

The intrinsic characteristics of spray-dried powders used to manufacture large ceramic slabs vary significantly overall, defining two classes in terms of agglomerate size distribution. Coarser-grained bodies have, on average, a higher amount of moisture and irregularly-shaped granules when compared to finer-grained powders.

Spray-dried bodies behave as free-flowing powders during die filling or deposition on tape. They are characterised by a rather narrow range of static angle of repose (25-34°), Hausner ratio (1.07-1.17) and mass flow (13-16 $g{\cdot}cm^{-2}{\cdot}s^{-1}$). These rheological properties do not appear to be strictly correlated, due to the narrow range of data and their experimental uncertainty, which suffers from a high degree of subjectivity in the rheological measurements.

The intrinsic characteristics of powders affect their flowability by the occurrence of coarser aggregates, particularly those irregular in shape, which are formed by coalescence of two or more individual agglomerates. For instance, the lower the amount of "popcorn"-shaped granules, the better the powder flowability.

These observations put in evidence the importance of quality control during spray drying and powder management. The formation of coarser aggregates should be avoided, preventing water vapour condensation and dripping in the spray drier as well as dripping in transportation and storage. Particular attention should be paid in re-moisturising operations.

The compaction of spray-dried granules determines a continuous change in the amount and typology of pores present in the green compact. Different slopes in the compaction curve reflect the varying work needed to compress first the intergranular pores (P_3) and the internal cavity of agglomerates (P_{2a}) and then, the coarser intragranular micro-porosity (P_{1b}) and the internal funnel of agglomerates (P_{2b}). Only the "incompressible" intragranular micro-porosity (P_{1a}) is present in the pressed tiles. The low-P regime (below ~10 MPa) fulfils a fast compression (approximately 80% of the bulk density gain), while the high-P regime acts progressively with a slow increase of bulk density.

Porcelain stoneware bodies used to manufacture large slabs exhibit a similar compressibility (Carr index mostly in the 50-55% range). Although there is a globally limited variance, the fact that the degree of compaction depends primarily on the moisture content must be taken into consideration. This implies—since all bodies have a moisture distribution in function of the agglomerate size—that bulk density can vary at the scale of the agglomerate dimension, particularly in case of coarse and irregularly-shaped granules.

Differences in the bulk density of unfired tiles are not retained in the finished product, as less dense green compacts sinter faster than denser ones. It means that any difference in the green bulk density turns into a different shrinkage during firing. Such differential shrinkages are the main cause of permanent deformations and residual stress in the large slabs.

6. ACKNOWLEDGEMENTS

Authors thank the Emilia-Romagna Region for financial support through the project IPERCER "Process Innovation for the Value Chain of the Sustainable Ceramic Tile" (CUP E32I16000010007), POR FESR 2014-2020 (Axis 1, Action 1.2.2).

7. REFERENCES

[1] García-Ten, J., Sánchez, E., Mallol, G., Jarque, J. C., & Arroyo, A. (2004). Influence of operating variables on spray-dried granule and resulting tile characteristics. In Key Engineering Materials, 264, 1499-1502.

[2] Amorós, J. L., Cantavella, V., Jarque, J. C., & Felíu, C. (2008). Fracture properties of spray-dried powder compacts: effect of granule size. Journal of the European Ceramic Society, 28(15), 2823-2834.

[3] Raimondo, M., Dondi, M., Zanelli, C., Guarini, G., Gozzi, A., Marani F., & Fossa, L. (2010). Boletín de la Sociedad Española de Cerámica y Vidrio, 49 (4), 289-295.

[4] Bresciani, A., & Ricci, C. (2008). Technologie de pressage Continua®. L'Industrie Céram. & Verrière, 1016, 24-28.

[5] Romagnoli, M., & Bignami, F. (2006). Study of the effect of additives on the flowability of ceramic powders. In Qualicer 2006. IX World Congress on Ceramic Tile Quality. (Vol. 3).

[6] Nebelung, M., & Lung., B. (2009). Flowability of ceramic bulk materials part 1: methods. Ceramic Forum International, 86, E35-E40.

[7] Amorós, J. L., Mallol, G., Feliu, C., & Orts, M. J. (2011). Study of the rheological behaviour of monomodal quartz particle beds under stress. A model for the shear yield functions of powders. Chemical engineering science, 66(18), 4070-4077.

[8] Santomaso, A., Lazzaro, P., & Canu, P. (2003). Powder flowability and density ratios: the impact of granules packing. Chemical Engineering Science, 58(13), 2857-2874.

[9] Geldart, D., Abdullah, E. C., Hassanpour, A., Nwoke, L. C., & Wouters, I. (2006). Characterisation of powder flowability using measurement of angle of repose. China Particuology, 4(3-4), 104-107.

[10] Zhou, Y. C., Xu, B. H., Yu, A. B., & Zulli, P. (2002). An experimental and numerical study of the angle of repose of coarse spheres. Powder technology, 125(1), 45-54.

[11] Wong, A. C. Y. (2002). Use of angle of repose and bulk densities for powder characterisation and the prediction of minimum fluidisation and minimum bubbling velocities. Chemical engineering science, 57(14), 2635-2640.

[12] Mellmann, J. (2001). The transverse motion of solids in rotating cylinders—forms of motion and transition behavior. Powder Technology, 118(3), 251-270.

[13] Abdullah, E. C., & Geldart, D. (1999). The use of bulk density measurements as flowability indicators. Powder technology, 102(2), 151-165.

[14] Mallol, G., Amoros, J. L., Orts, M. J., & Llorens, D. (2008). Densification of monomodal quartz particle beds by tapping. Chemical Engineering Science, 63(22), 5447-5456.

[15] Amorós, J. L., Orts, M. J., Garcia-Ten, J., Gozalbo, A., & Sánchez, E. (2007). Effect of the green porous texture on porcelain tile properties. Journal of the European Ceramic society, 27(5), 2295-2301.

[16] Reed, J. S. (2000). From batch to pressed tile: mechanics and system microstructural changes. Qualicer 2000, 1, Con23-42.

[17] Alves, H. J., Melchiades, F. G., & Boschi, A. O. (2010). Effect of spray-dried powder granulometry on the porous microstructure of polished porcelain tile. Journal of the European Ceramic Society, 30(6), 1259-1265.

[18] Zanelli C., Raimondo M., Guarini G., Marani F., Fossa L., Dondi M., Porcelain stoneware large slabs: processing and technological properties. Proc. 11th World Congress on Ceramic Tile Quality, QUALICER 2010, Castellón (Spain), p. 10.

[19] da Silva, A. L., Feltrin, J., Dal Bó, M., Bernardin, A. M., & Hotza, D. (2014). Effect of reduction of thickness on microstructure and properties of porcelain stoneware tiles. Ceramics International, 40(9), 14693-14699.

[20] Lukasiewicz, S. J. (1989). Spray-Drying Ceramic Powders. Journal of the American Ceramic Society, 72(4), 617-624.

[21] Niesz, D. E. (1996). A review of ceramic powder compaction. KONA Powder and Particle Journal, 14, 44-51.

[22] Beltrán, V., Ferrer, C., Bagán, V., Sánchez, E., Garcia, J., & Mestre, S. (1996). Influence of pressing powder characteristics and firing temperature on the porous microstructure and stain resistance of porcelain tile. IV World Congress on Ceramic Tile Quality, Castellon, Spain, Vol. 10, No. 13.

[23] SACMI (2001). Ceramic Technology. Editrice La Mandragora, Imola, ISBN 88-88108-16-5.

[24] Gil, C., Silvestre, D., García Ten, F. J., Quereda, M. F., & Vicente, M. J. (2012). Preparation of porcelain tile granulates by more environmentally sustainable processes. Bol. Soc. Esp. Ceram. Vidr. Vol 51. 2, 67-74,

[25] Shu, Z., Garcia-Ten, J., Monfort, E., Amoros, J. L., Zhou, J., & Wang, Y. X. (2012). Cleaner production of porcelain tile powders. Granule and green compact characterisation. Ceramics International, 38(1), 517-526.

[26] Kennedy, T., Hampshire, S., & Yaginuma, Y. (1997). A study of the compaction mechanism of granulated materials. Journal of the European Ceramic Society, 17(2-3), 133-139.

[27] Liu, D. M., Lin, J. T., & Tuan, W. H. (1999). Interdependence between green compact property and powder agglomeration and their relation to the sintering behaviour of zirconia powder. Ceramics international, 25(6), 551-559.

[28] Sanchez, E., Garcia, J., Barba, A., & Feliu, C. (2000). Effet de la composition des carreaux porcelainés sur le comportement au pressage de la poudre séchée par atomisation. L'Industrie Céramique & Verrière, (962), 539-541

[29] Celik, H. (2011). Effect of spray-dried powder granularity on porcelain tile properties. Journal of Ceramic Processing Research, 12(4), 483-487.

[30] Shu, Z., Garcia-Ten, J., Monfort, E., Amoros, J. L., Zhou, J., & Wang, Y. X. (2012). Cleaner production of porcelain tile powders. Fired compact properties. Ceramics International, 38(2), 1479-1487.

[31] Pérez, J. M., Rincón, J. M., & Romero, M. (2012). Effect of moulding pressure on microstructure and technological properties of porcelain stoneware. Ceramics International, 38(1), 317-325.

[32] Santos-Barbosa, D., Hotza, D., Boix, J., & Mallol, G. (2013). Modelling the influence of manufacturing process variables on dimensional changes of porcelain tiles. Advances in Materials Science and Engineering, 2013, ID 142343, 12 pages.

[33] Liu, S., & Ha, Z. (2002). Prediction of random packing limit for multimodal particle mixtures. Powder technology, 126(3), 283-296.

[34] Liu, D. M., & Lin, J. T. (1999). Influence of ceramic powders of different characteristics on particle packing structure and sintering behaviour. Journal of materials science, 34(8), 1959-1972.

[35] Tiscar, J. M., Escrig, A., Mallol, G., Pascual, N., Gilabert, F. A., Bonaque, R., & Pérez, J. A. (2016). Simulation of powder rheological behaviour in the ceramic tile pressing process. Qualicer 2016, XIV World Congress on Ceramic Tile Quality, Castellón, p. 1-13.

[36] Tiscar, J. M., Escrig, A., Mallol, G., Boix, J., & Gilabert Villegas, F. A. (2016). Influence of the die filling parameters during the ceramic tile pressing process via Discrete Element Method (DEM). 6th International Conference on Shaping of Advanced Ceramics (Shaping-VI).

[37] Zanelli, C., Ardit, M., Conte, S., Soldati, R., Cruciani, G., Dondi M. (2018). Viscous flow sintering of porcelain stoneware revisited. Proc. 15th World Congress on Ceramic Tile Quality, QUALICER 2018, Castellón (Spain), p. 9.

[38] Cantavella Soler, V., García Ten, F. J., Sánchez Vilches, E. J., Bannier, E., Sánchez, J., Sales, J. (2008). Delayed curvatures in porcelain tiles: analysis and measurement of incluencing factors. Proc. 10th World Congress on Ceramic Tile Quality, QUALICER 2008, Castellón (Spain).

[39] Bannier, E., García-Ten, J., Castellano, J., & Cantavella, V. (2013). Delayed curvature and residual stresses in porcelain tiles. Journal of the European Ceramic Society, 33(3), 493-501.

[40] Melchiades, F. G., Boschi, A. O., dos Santos, L. R., Dondi, M., Zanelli, C., Paganelli, M., & Mercurio, V. (2014). An insight into the pyroplasticity of porcelain stoneware tiles. Proc. 13th World Congress on Ceramic Tile Quality, QUALICER 2018, Castellón (Spain), p. 11.